Quantum-well states in ultrathin Ag(111) films deposited onto H-passivated Si(111)-(1×1) surfaces

A. Arranz,[1,2] J. F. Sánchez-Royo,[1,3] J. Avila,[1,4] V. Pérez-Dieste,[1,4] P. Dumas,[1] and M. C. Asensio[1,4,*]
[1]*LURE, Centre Universitaire Paris-Sud, Bât. 209 D, B.P. 34, 91898 Orsay Cedex, France*
[2]*Departmente de Física Aplicada, Facultad de Ciencias, C-XII, Universidad Autónoma de Madrid, Cantoblanco, 28049 Madrid, Spain*
[3]*Departmente de Física Aplicada, ICMUV, Universitat de Valencia, c/Dr. Moliner 50, 46100 Burjassot, Valencia, Spain*
[4]*Instituto de Ciencia de Materiales de Madrid, CSIC, Cantoblanco, 28049 Madrid, Spain*
(Received 5 June 2001; revised manuscript received 10 December 2001; published 24 April 2002)

Ag(111) films were deposited at room temperature onto H-passivated Si(111)-(1×1) substrates, and subsequently annealed at 300 °C. An abrupt nonreactive Ag/Si interface is formed, and very uniform nonstrained Ag(111) films of 6–12 ML have been grown. Angle-resolved photoemission spectroscopy was used to study the valence band electronic properties of these films. Well-defined Ag *sp* quantum-well states (QWS's) have been observed at discrete energies between 0.5–2 eV below the Fermi level, and their dispersions have been measured along the $\overline{\Gamma K}$, $\overline{\Gamma M(M')}$, and ΓL symmetry directions. QWS's show a parabolic bidimensional dispersion, with in-plane effective mass of $(0.38–0.50)m_o$, along the $\overline{\Gamma K}$ and $\overline{\Gamma M(M')}$ directions, whereas no dispersion has been found along the ΓL direction, indicating the low-dimensional electronic character of these states. The binding energy dependence of the QWS as a function of the Ag film thickness has been analyzed in the framework of the phase accumulation model. A good agreement between experimental data and the above-mentioned model is obtained for the Ag/H/Si(111)-(1×1) system. Hydrogen at the interface not only enhances the Ag film uniformity, but also acts as a barrier modifying the phase change of the Ag-*sp* electron wave upon reflection at the Ag/Si interface.

DOI: 10.1103/PhysRevB.65.195410 PACS number(s): 73.21.−b, 79.60.−i, 81.07.−b

I. INTRODUCTION

During the last years, the study of low-dimensional structures has attracted considerable interest because spatial confinement of electrons in thin films results in discrete quantum-well states (QWS's). In semiconductor layer systems, these effects are well known, and they have already been used in electronic devices. However, the observation of quantization effects in metallic layers has been restricted to a few systems. In this respect, thin Ag films have attracted a great interest due to the nearly free-electron characteristics of the *sp* bands over large regions of the Brillouin zone (BZ). Ag-*sp* QWS's have been widely observed in thin Ag films deposited onto several metallic substrates.[1–14] In contrast, confinement effects on Ag films deposited onto semiconductor substrates have been only observed in a scarce number of systems.[15–18] Weak peaks associated to QWS's have been observed by Wachs *et al.*[15] in photoemission spectra of 5–15 ML Ag films deposited on Si(111)-(7×7) at room temperature (RT). The weakness of the QWS's observed by these authors could be associated with the formation of a nonuniform Ag island size distribution, which would wash out the manifestation of quantum size effects in photoemission. These facts suggest that an improvement of Ag deposition conditions and silicon substrate preparation could play a key role for the observation of well-defined QWS's in thin Ag films deposited onto silicon substrates. In fact, this was observed by Neuhold and Horn,[17] on a 21-ML Ag film deposited at 130 K onto a Si(111)-(7×7) substrate, and subsequently annealed at RT, and by Matsuda *et al.*[18] on 6–30-ML Ag films deposited at 100 K onto Si(001)-(2×1) substrates, after annealing at 300–450 K. Such special deposition conditions lead to the formation of more uniform Ag films, where quantum-size effects have been observed by photoemission. However, for the Si(111)-(7×7) substrates, strain induced by film growth was also present in the film.[17] Therefore, it would be desirable from both fundamental and technological point of views to consider alternative better Si(111) surfaces free of complex reconstruction structures, which could lead to the formation of high-quality non-strained Ag(111) films on Si(111) substrates.

The nucleation and growth mode of thin Ag films deposited onto Si surfaces can be modified by changing the surface free energy of the substrate. This modification can be accomplished by the termination of the Si(111) surface by a foreign atom.[19,20] For this reason, there is a great interest in the formation of high-quality artificially H-terminated Si(111)-(1×1) surfaces, by both a wet chemical treatment and an atomic hydrogen-based method.[21] Hydrogenation of the Si(111)-(7×7) surface saturates the dangling bonds, restoring the 1×1 symmetry of bulk silicon. In a recent study on the electronic structure of the H-terminated Si(111)-(1×1) surface, the high quality of such a type of unreconstructed Si surfaces prepared by a wet chemical treatment has been confirmed by angle-resolved photoemission spectroscopy (ARPES).[22] Four remarkably sharp features have been resolved in the valence-band photoemission spectra at the $\overline{K}$ point, being attributed to (i) a surface resonance with a p_x-p_y symmetry, (ii) a surface state identified as a Si-Si backbond state, and (iii) two different higher binding-energy H-Si surface states.

The growth mode and structure of thin Ag films deposited onto hydrogen passivated silicon surfaces are substantially different from the observed ones for Si(111)-(7×7) sur-

faces.[19,20] When Ag is deposited onto a clean Si(111)-(7×7) surface, the growth proceeds in a quasi-layer-by-layer mode at RT, and according to the Stranski-Krastanov growth mode at 300 °C. Opposite to this, Ag deposition at 300 °C onto the H/Si(111)-(1×1) surface, leads to a quasi-layer-by-layer growth mode. In this case, the formation of islands much thinner and with a narrower size distribution than those on the nonpassivated substrate was observed by impact-collision ion-scattering spectroscopy[19] and scanning electron microscopy.[20,23] In addition, Sumitomo *et al.*[19] have found that Ag films deposited onto Si(111)-(7×7) substrates at RT have a two-domain Ag(111) island distribution, whereas those grown on the hydrogen-terminated surface at 300 °C have a single-domain preferred orientation. According to these authors, hydrogen-mediated epitaxy of single-domain Ag(111) films deposited on Si(111)-(7×7) substrates at 300 °C is observed. It has been suggested that hydrogen at the interface can be partially removed during Ag deposition at high temperatures.[24–26] If the hydrogen coverage at the interface would decrease below 0.3 ML, an undesired reconstruction of the surface, to a two-dimensional layer of the Si(111)$\sqrt{3}\times\sqrt{3}$-Ag structure, plus thicker Ag(111) islands could occur.[24,27] So it would be desirable to lower the Ag temperature deposition in order to avoid a significant hydrogen elimination at the interface, and therefore the above-mentioned surface reconstruction.

Ag deposition at RT onto hydrogen-terminated Si(111) surfaces has only been studied by scanning tunneling microscopy (STM)[27,28] and by low-energy electron diffraction (LEED).[24] LEED patterns[24] show that hydrogen termination remarkably suppresses the rotational disorder of Ag(111) films which is observed for Ag deposition on Si(111)-(7×7) surfaces. In addition, a decrease of the average size of the Ag islands along with an increase of the island density, have been found by STM upon decreasing the substrate temperature from 300 °C to RT.[27] Therefore, RT deposition leads to even more uniform and compact Ag films than those deposited at higher temperatures. Unfortunately, in the literature there is a lack of information from structural techniques about the single- or two-domain preferred orientation of thin Ag films deposited on hydrogen-terminated Si substrates at RT. Recently, the above-mentioned subject has been addressed by studying the Fermi surface (FS) of 6-ML Ag films deposited onto H-passivated Si(111)-(1×1) surfaces at RT, and subsequently annealed at 300 °C.[29] This study has shown that the measured FS reflects a sixfold symmetry rather than the threefold symmetry expected for a Ag(111) single crystal. This behavior confirmed the fact that these Ag films are composed by two domains rotated 60°, being the first evidence of a two-domain preferred orientation of the Ag(111) films deposited at RT onto H-terminated Si(111)-(1×1) surfaces.

In this work, thin Ag(111) films have been deposited in ultrahigh-vacuum (UHV) at RT onto H-passivated Si(111)-(1×1) substrates, and subsequently annealed at 300 °C to enhance the film uniformity. In such a way, an abrupt nonreactive Ag/Si interface is formed, and very uniform nonstrained thin Ag(111) films of 6–12 ML have been obtained. The high quality of the silver films has been probed by ARPES. Well-defined Ag *sp* QWS's have been observed at discrete energies between 0.5 and 2 eV below the Fermi level (E_F), and their energy dispersions have been measured along the $\overline{\Gamma K}$, $\overline{\Gamma M(M')}$ and ΓL symmetry directions. QWS's show a parabolic dispersion, with an in-plane effective mass of $(0.38–0.50)m_o$, along the $\overline{\Gamma K}$ and $\overline{\Gamma M(M')}$ symmetry directions, whereas no dispersion has been found along the ΓL direction, supporting the two-dimensional electronic character of these states. On the other hand, the binding energy dependence of the QWS's as a function of Ag film thickness has been analyzed in the framework of the phase accumulation model.[4] A good agreement between experimental data and the above-mentioned model is obtained for the Ag/H/Si(111)-(1×1) system.

II. EXPERIMENTAL DETAILS

The experiments were performed at LURE (Orsay, France) using the French-Spanish (PES2) experimental station of the Super-Aco storage ring, described elsewhere.[30] The measurements were carried out in a purpose-built UHV system, with a base pressure of 5×10^{-11} mbar, equipped with an angle resolving 50-mm hemispherical VSW analyzer coupled on a goniometer inside the chamber. The manipulator was mounted in a two-axis goniometer that allows rotation of the sample in (i) the whole 360° azimuthal angle (ϕ), and (ii) in the 180° polar emission angle relative to surface normal (θ), with an overall angular resolution of 0.5°. The current incident angle of the light (Θ_i) was 45°.The available energy of light ($h\nu$) was between 18 and 150 eV. For a photon energy of 32 eV, the overall energy resolution, including the analyzer, was 60 meV.[22]

The substrate was an *n*-doped Si(111) single crystal, with a nominal resistivity of 100 Ω cm. It was prepared *ex situ* using a wet chemical treatment that results in a passivated H/Si(111)-(1×1) surface.[21] After introducing the substrate in the analysis chamber, the quality of the surface was checked out through the sharpness of the features appearing in the valence-band photoemission spectrum at the $\overline{K}$ point, which are attributed to intrinsic H-Si surface states.[22] Ag was evaporated onto the surface at RT. The rate of evaporation, 0.06±0.002 ML/min, was determined by using a quartz microbalance. In these conditions, Ag films of thicknesses ranging from 6 to 12 ML were deposited onto H/Si(111)-(1×1) surfaces at RT, and subsequently annealed at 300 °C to enhance the film uniformity.

III. RESULTS AND DISCUSSION

Normal and off-normal valence-band (VB) photoemission spectra, after background subtraction, of 6–12-ML Ag films deposited at RT onto H-terminated Si(111)-(1×1) substrates and subsequently annealed at 300 °C, are presented in order to obtain the Ag *sp*-band dispersion along the ΓL, $\overline{\Gamma K}$, and $\overline{\Gamma M(M')}$ symmetry directions. Figure 1 shows the evolution of the normal-emission VB spectra measured with $h\nu=32$ eV as a function of Ag thickness. The intense and sharp peak observed at 0.1eV below E_F is the surface state (SS) in the band gap along the direction of the Ag(111) crys-

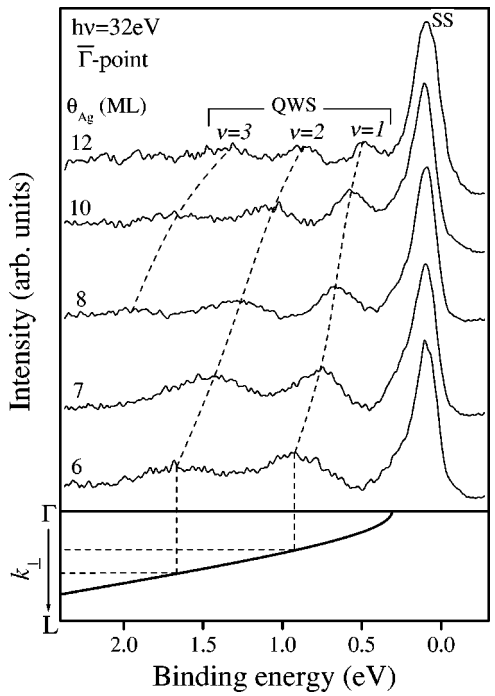

FIG. 1. Normal-emission valence-band spectra measured with $h\nu=32$ eV for different Ag film thicknesses deposited onto an H-terminated Si(111)-(1×1) substrate at RT, and subsequently annealed at 300 °C. In the bottom, the sp band dispersion $E(k_\perp)$ of bulk Ag along the ΓL direction is shown in order to illustrate the physical origin of the QWS peaks observed in the spectra.

tal. The sharpness of this peak reflects the good crystallinity and orientation of the Ag film. It should be pointed out that the sharpness observed for this peak is comparable to the observed one for Ag films deposited onto highly oriented pyrolytic graphite, HOPG(0001), where a very narrow height distribution of Ag islands has been observed.[5,17] Neuhold and Horn[17] have attributed the depopulation of the Ag SS to the presence of tensile strain induced by film growth in a 21-ML Ag film on Si(111)-(7×7). Comparison of our results with the works of Wachs *et al.*[15] and Neuhold and Horn[17] suggests an improvement of the quality of the silver films, as a consequence of the ideally H-terminated Si(111) substrate surface used in this work. As a consequence, high-quality nonstrained Ag films can be successfully prepared onto H-passivated Si(111)-(1×1) surfaces at RT, with a subsequent annealing. Alternative techniques for Ag deposition on Si(111), based on the cooling of the substrate to 130 K and subsequent annealing at RT, also lead to the formation of very uniform Ag films where manifestation of quantum-size effects in photoemission has been observed.[17] However, effects associated with the strain cannot be avoided, and should be taken into account to describe the electronic properties of such Ag thin films.[17]

Three series of well-resolved intense Ag sp QWS's, characterized by the quantum number $\nu=1-3$, can be observed at discrete energies between 0.5 and 2 eV below the Fermi level in Fig. 1. The evolution of the QWS energies as a function of Ag thickness for the different series observed ($\nu=1$, 2 and 3) will be analyzed later in the backdrop of the phase accumulation model, (PAM).[4] The quantum number ν is defined as $\nu=m-n$, where m is the number of Ag monolayers, and n is the number of antinodes in the probability density. Ag sp QWS's of similar quality have been also observed by Neuhold and Horn[17] in a 21-ML Ag film on Si(111)-(7×7), deposited at 130 K and subsequently annealed at RT, suggesting that special Ag deposition conditions, or as shown in this work, Si(111) substrates free of complex surface reconstructions, are necessary in order to observe quantum-size effects in Ag films deposited onto Si(111) substrates. Therefore, it should be pointed out that the weakness of the QWS peaks observed by Wachs *et al.*[15] in the photoemission spectra of 5–15-ML Ag films deposited at RT onto Si(111)-(7×7) should be associated with the formation of a nonuniform Ag island size distribution, as a consequence of standard deposition at RT. STM studies have shown that Ag deposition on Si(111)-(7×7) substrates at RT produces three-dimensional structures that are far from an ideal epitaxial film.[31,32] In the lower part of Fig. 1, the sp-band dispersion $E(k_\perp)$ of bulk Ag along the ΓL direction is shown in order to illustrate the physical origin of the QWS peaks observed in the spectra. The above-mentioned dispersion relation $E(k_\perp)$ has been simulated by the two-band model given by Eq. (1),[5]

$$E(k_\perp)=E_o-A(k_{BZ}-k_\perp)^2+U-\sqrt{4A^2B(k_{BZ}-k_\perp)^2+U^2}, \tag{1}$$

where $A=\hbar^2/2m^*$, $B=3\pi^2/a^2$, $a=4.09$ Å is the silver lattice constant, $U=4.2$ eV is the width of the gap at the L symmetry point of Ag(111), $E_o=0.31$ eV is the position of the sp-band edge relative to E_F, $m^*=0.7m_o$ is the effective mass of the electrons in this band, (m_o being the free-electron mass), and $k_{BZ}=1.33$ Å^{-1} is the wave vector at the BZ boundary (the L point in the [111] direction).

Angle-resolved photoemission spectra of the VB measured with $h\nu=32$ eV, along the $\overline{\Gamma K}$ and $\overline{\Gamma M(M')}$ symmetry directions are presented in Figs. 2 and 3, for 6- and 7-ML Ag films, respectively. As a reference, a scheme of the Ag(111) surface reciprocal-lattice unit cell is shown in the figures. It should be pointed out, that $\overline{M}$ and $\overline{M'}$ points of the surface BZ overlap because Ag films are composed by two 60° rotated domains from each others.[29] Dashed lines have been added to show the energy dispersion of the different peaks observed in the spectra. These peaks are the QWS's denoted by $\nu=1$ and 2 in Fig. 1, and the feature associated with the Ag(111) surface state. The insets of Figs. 2 and 3 show the band diagram extracted from the dispersion of these features. Solid lines are parabolic fits to Eq. (2), that are expected to be a good approximation for small parallel wave vector, $k_\parallel$, values:[2]

$$E_\nu(k_\parallel)=E_\nu(k_\parallel=0)+\hbar^2k_\parallel^2/2m_\parallel^*. \tag{2}$$

In Eq. (2), $E_\nu(k_\parallel=0)$, and the in-plane effective mass $m_\parallel^*$, are fitting parameters.

In agreement with a previous work,[29] two sp Ag-derived surface states SS1 and SS2, at binding energies of ~0.1 and 0.32 eV, respectively, are found in the gap along the ΓL direction of the Ag(111) films. The existence of two different

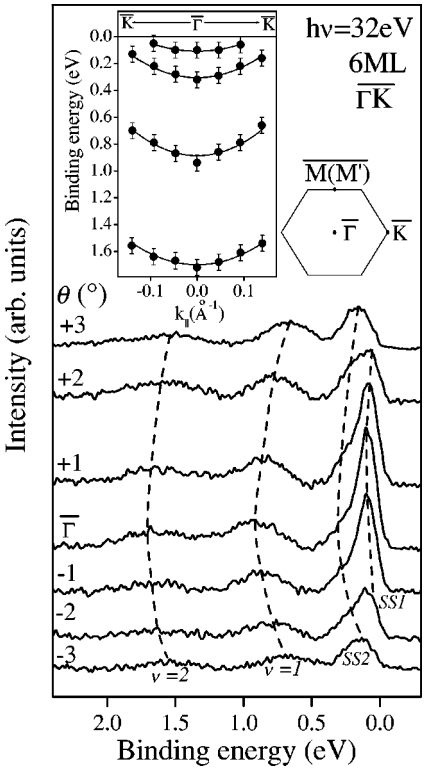

FIG. 2. Angle-resolved photoemission spectra of the VB measured with $h\nu = 32$ eV along the $\overline{\Gamma K}$ symmetry direction for the 6-ML Ag film of Fig. 1. As a reference, a scheme of the Ag surface reciprocal-lattice unit cell is given in the figure. The inset shows the band diagram extracted from the dispersion of the features observed in the spectra.

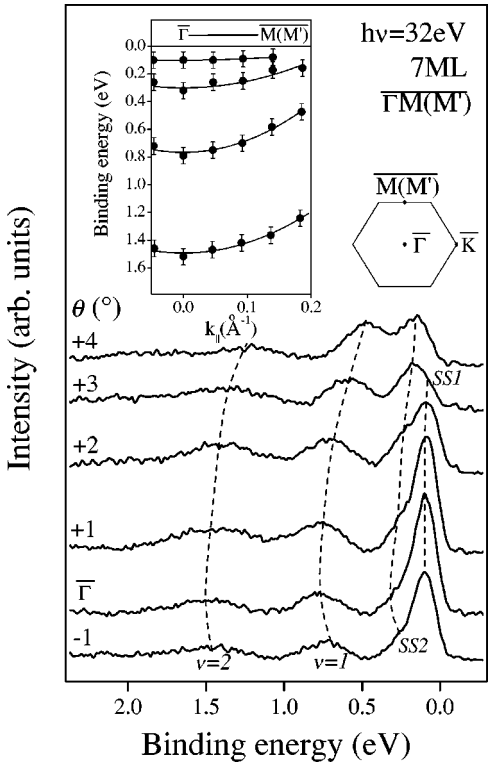

FIG. 3. Angle-resolved photoemission spectra of the VB measured with $h\nu = 32$ eV along the $\overline{\Gamma M(M')}$ symmetry direction for the 7-ML Ag film of Fig. 1. As a reference, a scheme of the Ag surface reciprocal-lattice unit cell is given in the figure. The inset shows the band diagram extracted from the dispersion of the features observed in the spectra.

surface states with the same origin was attributed to the inhomogeneous presence of hydrogen at the interface, due to the fact that the annealing process partially removes hydrogen; therefore, a downshift of the Ag surface state is produced in regions where hydrogen still remains at the interface. It should be noted, that for Ag film thicknesses $\geqslant 6$ ML, the SS2 feature appears as an asymmetry of the more intense SS1 peak in normal-emission spectra. However, the SS2 peak becomes clearly resolved in the off-normal-emission spectra of Figs. 2 and 3, as a consequence of the Fermi level crossing of the SS1 state.

Surface states and QWS's show a parabolic in-plane dispersion, as can be observed in the insets of Figs. 2 and 3. The QWS in-plane effective mass $m_{\parallel}^{*}$ has been obtained from the fit of experimental data to Eq. (2), giving values between $0.38m_o$ and $0.50m_o$. These values are in good agreement with the reported ones in the literature for silver films on Cu(111) substrates, and are almost the same as the effective mass for the Ag sp valence band derived from a band-structure calculation.[2,9] Moreover, a linear increase of the in-plane effective mass with the binding energy has been observed. A similar behavior was also found by Mueller *et al.* for the Ag/Cu(111) quantum-well system.[2]

The evolution of the normal emission VB spectra as a function of $h\nu$ for a 7-ML Ag(111) film is presented in Fig. 4. As can be observed, a negligible dispersion is found for QWS's along the ΓL symmetry direction, as a consequence of the quantization of the perpendicular wave-vector component, $k_{\perp}$, due to the finite and homogeneous thickness of the film. The nondispersive behavior along the ΓL direction, and the parabolic in-plane dispersion along the $\overline{\Gamma K}$ and $\overline{\Gamma M(M')}$ symmetry directions of the QWS and surface states, indicate the two-dimensional electronic character of these states.

The observation of confinement effects in the Ag/H/Si(111)-(1×1) system requires either the presence of a relative gap in the Si(111) substrate, or the presence of a so-called symmetry or hybridization gap, in order to avoid the coupling of Ag-sp states with Si(111) sp states of similar symmetry.[1] Well-defined QWS's have been observed in this work for energies between 0.5 and 2 eV below E_F. Neuhold and Horn[17] have also observed similar quality QWS's up to an energy of 3 eV below E_F. Thus, the above-mentioned requirements should be fulfilled for hydrogen-passivated and -nonpassivated Si(111) substrates. According to the calculated valence-band structure,[22] the maximum of the valence band is at ~ 0.8 eV below E_F [for n-doped Si(111) substrates], and the first occupied state at the $\overline{\Gamma}$ point has been observed at ~ 1.2 eV below E_F for the H-Si(111)-(1×1) surface.[29] In addition, a Si band bending of $\sim$-0.2 eV, calculated using a value of 0.5 eV for the Schottky barrier corrected according to the interface-dipole model, should also be considered.[33,34] Therefore, the gap at the $\overline{\Gamma}$ point in the

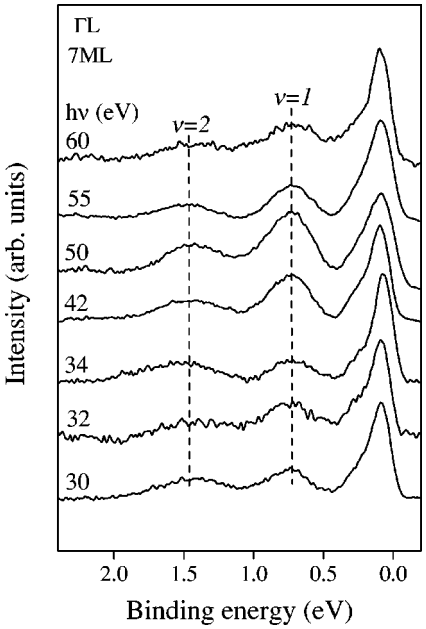

FIG. 4. Normal-emission valence-band spectra as a function of the energy of light, $h\nu$, for the 7-ML Ag film of Fig. 1.

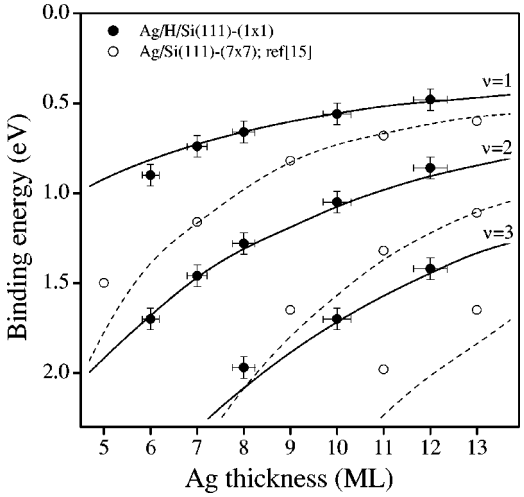

FIG. 5. QWS binding energies of Fig. 1 as a function of Ag film thickness (solid symbols). For comparison, data corresponding to 5–13-ML Ag films deposited onto Si(111)-(7×7) at RT, extracted from Ref. 15, have been also plotted (open symbols). Dashed lines are the calculated thickness dependence of the QWS binding energies according to the phase accumulation model proposed in the text.

[111] direction of the Ag-deposited H-Si(111)-(1×1) substrate extends up to ~1 eV below E_F. So the observation of QWS's for binding energies above 1 eV, should be explained by the lack of coupling between the Ag-sp states and the Si(111) bulk states. The role of the presence of hydrogen at the Ag/Si(111) interface should also be taken into account. It could act as a barrier, that would enhance the inhibition of the above-mentioned coupling, as observed in the 15-ML Ag+x-ML Au + Ag(111) quantum-well system, upon increasing the Au interlayer thickness from $x=0$ to 3 ML.[7]

In order to further analyze the dependence of the QWS energies with the Ag film thickness, the binding energies of the QWS's observed in Fig. 1 are plotted (solid symbols) as a function of the Ag film thickness in Fig. 5. In this figure, data corresponding to 5–13-ML Ag films deposited onto Si(111)-7×7 at RT (Ref. 15) have also been plotted for comparison (open symbols). According to the phase accumulation model,[4] the energy position of the QWS is given by Eq. (3),

$$2k_{\perp}(E)d+\Phi_C(E)+\Phi_B(E)=2\nu\pi, \qquad (3)$$

where $k_{\perp}(E)$ is the electron wave-vector component normal to the surface, d is the Ag film thickness, ν is the quantum number previously defined, and $\Phi_C(E)$ and $\Phi_B(E)$ are the phase shifts upon reflection of the electron wave function at the film/substrate and film/vacuum interfaces, respectively. The above-mentioned model considers that QWS's are electron waves trapped inside the Ag film between the barriers at the Ag/Si(111) and Ag/vacuum interfaces. Upon reflection of the Ag-sp electrons at the interfaces, phase changes $\Phi_C(E)$ and $\Phi_B(E)$ are introduced, whereas $k_{\perp}(E)d$ is the phase change accumulated upon traversing the Ag film. In this way, thin uniform Ag films can be considered as an electron interferometer,[35] where the electron undergoes multiple reflections between the interfaces. For a given Ag film thickness, an Ag-sp electron standing wave is expected at a discrete energy in the photoemission spectra, when the total phase change satisfies the condition given by Eq. (3). Figure 6 shows a schematic diagram illustrating the analogy of the phase accumulation model with an electron interferometer for the Ag/Si(111)-(1×1)-H system. Multiple reflection at the interfaces of Ag-sp electrons are indicated by dashed arrows. Ideal confinement is achieved for a 100% interface reflectivity. A reflectivity lower than 100% would imply partial transmission of the electron wave outside the Ag film as evanescent states, indicated by short arrows in the figure.

In Eq. (3), the dispersion relation $k_{\perp}(E)$ for Ag(111) in the ΓL direction can be simulated by the two-band model previously defined by Eq. (1). For Ag thin films deposited on HOPG(0001) and Fe(100) substrates,[4,5] $\Phi_C(E)$ has been de-

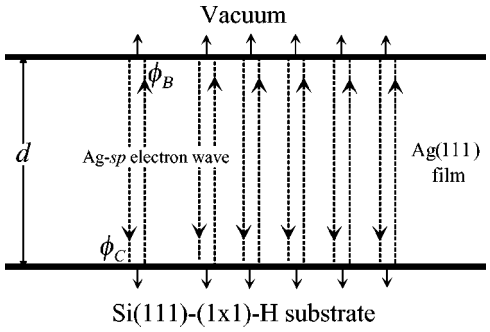

FIG. 6. Schematic diagram illustrating the analogy of the multiple-reflection phase accumulation model with an electron interferometer for the Ag/Si(111)-(1×1)-H system. Multiple reflections at the interfaces of Ag-sp electrons are indicated by dashed arrows. Evanescent states outside the Ag films, due to interface reflectivities lower than 100%, are indicated by short arrows.

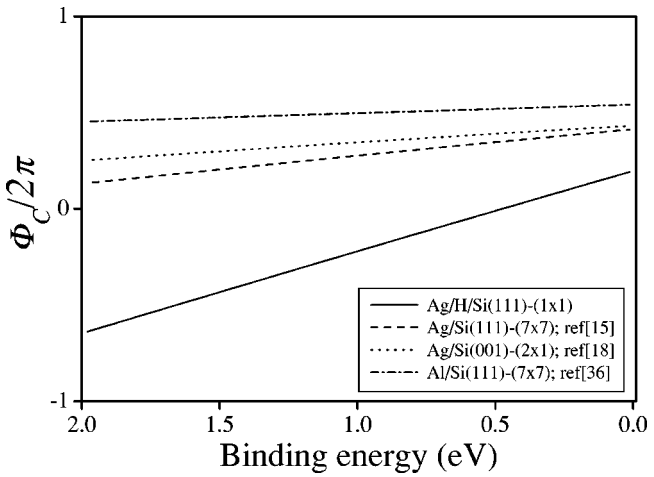

FIG. 7. $\Phi_C(E)/2\pi$ as a function of the binding energy, for the Ag/H/Si(111)-(1×1) (solid line), Ag/Si(111)-(7×7) (Ref. 15), (dashed line), Ag/Si(001)-(2×1) (Ref. 18), (dotted line), and Al/Si(111)-(7×7) (Ref. 36) (dash-dotted line) interfaces, respectively.

scribed by a semiempirical formula based on a step potential approximation, in such a way that $\Phi_C(E)$ varies from $-\pi$ to 0 from the bottom to the top of the gap.[4] However, such an approximation does not seem to be valid for the Ag/H/Si(111)-(1×1) system, where a combination of relative and symmetry gaps should be considered in order to account for the observed confinement effects. In addition, it should be pointed out that positive values for $\Phi_C(E)$ were recently obtained for the Ag/Si(001)-(2×1) and Al/Si(111)-(7×7) systems.[18,36] For this reason, we have assumed that the total phase $\Phi(E)=\Phi_B(E)+\Phi_C(E)$ is a linear function of E.[3,18,36] The solid lines in Fig. 5 represent the calculated thickness dependence of the binding energy of the QWS (with $\nu=1-3$) based on the fit of the experimental data (solid symbols) to the PAM proposed by Eq. (3). The best fit has been obtained for $\Phi(E)=0.75-2.86E$. The good agreement between experimental data and calculated lines suggests that the PAM can successfully characterize the QWS observed in the Ag/H/Si(111)-(1×1) system. The application of the PAM model to the data of the Ag/Si(111)-(7×7) system[15] (open symbols in Fig. 5) gives $\Phi(E)=2.13-1.13E$. The best fit for these data is shown as dashed lines.

As observed in Fig. 5, for a given Ag thickness, QWS's with the same quantum number ν are observed at lower binding energies in the Ag/H/Si(111)-(1×1) system than in the Ag/Si(111)-(7×7) one. To gain more insight about this fact, the phase change upon reflection of the Ag-sp electron wave at the Ag/substrate interface, $\Phi_C(E)=\Phi(E)-\Phi_B(E)$, has been calculated, using a semiempirical approximation for $\Phi_B(E)$.[4,18] Figure 7 shows $\Phi_C(E)/2\pi$ as a function of the binding energy, for the Ag/H/Si(111)-(1×1) (solid line), Ag/Si(111)-(7×7) (Ref. 16) (dashed line), and Ag/Si(001)-(2×1) (Ref. 18) (dotted line) interfaces, respectively. $\Phi_C(E)$ for the Al/Si(111)-(1×1) is also given for comparison (dash-dotted line).[36] For Ag/Si(111)-(7×7), Ag/Si(001)-(2×1) and Al/Si(111)-(7×7) interfaces, $\Phi_C(E)$ is positive, and varies smoothly with E. Opposite to this behavior, $\Phi_C(E)$ for the Ag/H/Si(111)-(1×1) is mainly negative, showing a pronounced increase in the energy range from 2 to 0 eV. This behavior resembles the negative phases obtained for the Ag(100)/Fe(100) interface, and other metal/metal interfaces.[3,12] According to Fig. 7, it seems that metal/semiconductor interfaces are characterized by a smooth-varying positive $\Phi_C(E)$, whereas for metal/metal interfaces a marked-varying negative $\Phi_C(E)$ has been found.[3,12] Therefore, metal/semiconductor and metal/metal interfaces have large differences in the phase change that an electron-wave undergoes at the interface, as pointed out by Matsuda *et al.*, for the scattering of Bloch states near the Fermi level.[18] However, $\Phi_C(E)$ of the Ag/H/Si(111)-(1×1) interface shows a behavior rather different that the expected for a metal/semiconductor inteface, being similar to the expected one for a metal/metal interface. This fact, suggests that hydrogen passivation of Si(111) substrate not only enhances the Ag film uniformity, but also changes the electron-wave scattering mechanism at the interface. This could be a consequence of the inhibiting electronic-coupling role of the hydrogen at the interface. Nevertheless, additional work should be done to get further information on $\Phi_C(E)$ changes induced by an atomic interlayer at metal/semiconductor interfaces.

IV. SUMMARY AND CONCLUSIONS

Thin Ag(111) films have been deposited in UHV at room temperature onto H-passivated Si(111)-(1×1) substrates, and subsequently annealed at 300 °C to enhance the film uniformity. Deposition onto H-terminated Si(111)-(1×1) unreconstructed surfaces suppresses strain induced by film growth. As a consequence, an abrupt nonreactive Ag/Si interface is formed, and very uniform nonstrained Ag(111) films of 6–12 ML have been obtained. The quality of the silver films has been probed by ARPES. Well-defined Ag-sp QWS's have been observed at discrete energies between 0.5–2 eV below the Fermi level, and their energy dispersion have been measured along the $\overline{\Gamma K}$, $\overline{\Gamma M(M')}$, and ΓL symmetry directions. QWS's show a parabolic dispersion, with in-plane effective mass of $(0.38-0.50)m_o$, along the $\overline{\Gamma K}$ and $\overline{\Gamma M(M')}$ directions, whereas no dispersion has been found along the ΓL direction, supporting the two-dimensional electronic character of these states.

On the other hand, the binding energy dependence of the QWS as a function of the Ag film thickness has been analyzed in the framework of the phase accumulation model. A good agreement between experimental data and the above-mentioned model is obtained for the Ag/H/Si(111)-(1×1) system. A comparison of our results with the works existing in the literature on QWS's on Ag/Si interfaces, suggests that hydrogen at the interface not only enhances the Ag film uniformity, but also modifies the phase change of the Ag-sp electrons at the Ag/Si interface. Hydrogen could act as a barrier that would inhibit the electronic coupling between Ag and Si sp states at the interface, therefore enhancing the degree of confinement of electrons in the Ag thin film.

ACKNOWLEDGMENTS

This work was financed by DGICYT (Spain) (Grant No. PB-97-1199) and the Large Scale Facilities program of the EU to LURE. Financial support from the Comunidad Autónoma de Madrid (Project No. 07N/0042/98) is also acknowledged. A.A. and J.F.S.-R. acknowledge financial support from the Ministerio de Educación y Cultura of Spain.

*Electronic address: asensio@lure.u-psud.fr

[1] T.-C. Chiang, Surf. Sci. Rep. **39**, 181 (2000), and references therein.
[2] M.A. Mueller, T. Miller, and T.-C. Chiang, Phys. Rev. B **41**, 5214 (1990).
[3] J.E. Ortega, F.J. Himpsel, G.J. Mankey, and R.F. Willis, Phys. Rev. B **47**, 1540 (1993).
[4] N.V. Smith, N.B. Brookes, Y. Chang, and P.D. Johnson, Phys. Rev. B **49**, 332 (1994).
[5] F. Patthey and W.D. Schneider, Phys. Rev. B **50**, 17 560 (1994).
[6] S. Crampin, S. De Rossi, and F. Ciccacci, Phys. Rev. B **53**, 13 817 (1996).
[7] W.E. McMahon, T. Miller, and T.-C. Chiang, Phys. Rev. B **54**, 10 800 (1996).
[8] T. Valla, P. Pervan, M. Milun, A.B. Hayden, and D.P. Woodruff, Phys. Rev. B **54**, 11 786 (1996).
[9] K. Takahashi, A. Tanaka, M. Hatano, H. Sasaki, S. Suzuki, and S. Sato, J. Electron Spectrosc. Relat. Phenom. **88-91**, 347 (1998).
[10] M. Milun, P. Pervan, B. Gumhalter, and D.P. Woodruff, Phys. Rev. B **59**, 5170 (1999).
[11] A.M. Shikin, D.V. Vyalikh, Yu.S. Dedkov, G.V. Prudnikova, V.K. Adamchuk, E. Weschke, and G. Kaindl, Phys. Rev. B **62**, R2303 (2000).
[12] J.J. Paggel, T. Miller, and T.-C. Chiang, Phys. Rev. B **61**, 1804 (2000).
[13] J.J. Paggel, T. Miller, D.-A. Luh, and T.-C. Chiang, Appl. Surf. Sci. **162-163**, 78 (2000).
[14] A. Tanaka, H. Sasaki, K. Takahashi, W. Gondo, S. Suzuki, and S. Sato, Appl. Surf. Sci. **169-170**, 168 (2001).
[15] A.L. Wachs, A.P. Shapiro, T.C. Hsieh, and T.-C. Chiang, Phys. Rev. B **33**, 1460 (1986).
[16] D.A. Evans, M. Alonso, R. Cimino, and K. Horn, Phys. Rev. Lett. **70**, 3483 (1993).
[17] G. Neuhold and K. Horn, Phys. Rev. Lett. **78**, 1327 (1997).
[18] I. Matsuda, H.W. Yeom, T. Tanikawa, K. Tono, T. Nagao, S. Hasegawa, and T. Ohta, Phys. Rev. B **63**, 125325 (2001).
[19] K. Sumitomo, T. Kobayashi, F. Shoji, K. Oura, and I. Katayama, Phys. Rev. Lett. **63**, 1193 (1991).
[20] K. Oura, V.G. Lifshits, A.A. Saranin, A.V. Zotov, and M. Katayama, Surf. Sci. Rep. **35**, 1 (1999).
[21] G.S. Higashi, Y.J. Chabal, G.W. Trucks, and K. Raghavachari, Appl. Phys. Lett. **56**, 656 (1990); G. S. Higashi, R. S. Becker, Y. J. Chabal, and A. J. Becker, *ibid.* **58**, 1656 (1991); P. Dumas, Y.J. Chabal, and G.S. Higashi, Phys. Rev. Lett. **65**, 1124 (1990).
[22] S. Gallego, J. Avila, L. Martin, X. Blase, A. Taleb, P. Dumas, and M.C. Asensio, Phys. Rev. B **61**, 12 628 (2000).
[23] M. Naitoh, F. Shoji, and K. Oura, Jpn. J. Appl. Phys. **31**, 4018 (1992).
[24] M. Naitoh, F. Shoji, and K. Oura, Surf. Sci. **242**, 152 (1991).
[25] A. Nishiyama, G. ter Horst, P.M. Zagwijn, G.N. Van der Hoven, J.W.M. Frenken, F. Garten, A.R. Schlatmann, and J. Vrijmoeth, Surf. Sci. **350**, 229 (1996).
[26] K. Fukutani, H. Iwai, Y. Murata, and H. Yamashita, Phys. Rev. B **59**, 13 020 (1999).
[27] Y. Ohba, I. Katayama, Y. Yamamoto, M. Watamori, and K. Oura, Appl. Surf. Sci. **113-114**, 448 (1997).
[28] M. Naitoh, A. Watanabe, and S. Nishigaki, Surf. Sci. **357-358**, 140 (1996).
[29] A. Arranz, J.F. Sánchez-Royo, J. Avila, V. Pérez-Dieste, P. Dumas, and M.C. Asensio, Phys. Rev. B **65**, 075405 (2002).
[30] J. Avila, C. Casado, M.C. Asensio, J.L. Pérez, M.C. Muñoz, and F. Soria, J. Vac. Sci. Technol. A **13**, 1501 (1995).
[31] St. Tosch and H. Neddermeyer, Phys. Rev. Lett. **61**, 349 (1988).
[32] L. Huang, S.J. Chey, and J.H. Weaver, Surf. Sci. **416**, L1101 (1998).
[33] T.U. Kampen and W. Mönch, Surf. Sci. **331-333**, 490 (1995).
[34] T.U. Kampen, R.F. Schimtsdorf, and W. Mönch, Appl. Phys. A: Mater. Sci. Process. **60**, 391 (1995).
[35] J. J. Paggel, T. Miller, and T.-C. Chiang, Science **283**, 1709 (1999).
[36] L. Aballe, C. Rogero, S. Gokhale, S. Kulkarni, and K. Horn, Surf. Sci. **482-485**, 488 (2001).